XLI CILAMCE
XLI Ibero-Latin American Congress on Computational Methods in Engineering
16-19 November, 2020 FOZ DO IGUAÇU PARANÁ - BRAZIL

Computational fluid dynamics of biomaterial inks flowing through extrusion nozzles in bioprinting of substitutes for cartilaginous tissues

Isabela M. Poley[1], Patrícia M. de Oliveira[2], Estevam B. Las Casas[2]

[1]*Bioengineering Laboratory (LABBIO), Universidade Federal de Minas Gerais*
6627, Presidente Antônio Carlos Ave., Belo Horizonte, CEP: 31270-901, Minas Gerais, Brazil
poley@ufmg.br
[2]*Biomechanical Engineering Group (MECBIO), Universidade Federal de Minas Gerais*
6627, Presidente Antônio Carlos Ave., Belo Horizonte, CEP: 31270-901, Minas Gerais, Brazil
munizpatricia@outlook.com, estevam@dees.ufmg.br

Abstract. Computational fluid dynamics (CFD) can be useful to predict the behavior of biomaterials in bioprinting in order to avoid clogging of extrusion nozzles and, in case of cell embedded biomaterials, to avoid wasting cells. In bioprinting, cells are exposed to high shear stresses when in contact against the printing needle walls. If the stresses exceed a limit value, cell membranes may disrupt. Biomaterial inks specially formulated for bioprinting of substitutes for cartilaginous tissues were characterized for their rheological properties, and the obtained data were used in fluid dynamics simulations of the flow through extrusion nozzles. Some compositions contained powdered extracellular matrix derived from devitalized cartilage (DVC), added to give the biochemical complexity necessary for the bioprinted material, and others contained polycaprolactone (PCL), added to give greater mechanical resistance. The simulations indicated very high shear stresses (greater than 4 kPa) during extrusion for compositions containing PCL, which could cause cell disruption in high extent. It is concluded that, for those compositions, the addition of cells to the scaffolds should be done preferably after bioprinting, instead of using a cell embedded biomaterial, because cell viability after extrusion tends to be low.

Keywords: bioprinting, biomaterial ink, bioink, CFD, rheology.

1 Introduction

This study describes the investigation of the flow behavior of different compositions of biomaterials using computational fluid dynamics (CFD). Those biomaterials were precursors of bioinks for bioprinting of three-dimensional substitutes of human cartilaginous tissues. Rheology data for each composition have been obtained and applied to the flow simulations through two different geometries of extruder nozzles.

The extrusion bioprinting systems considered in this study deposit biomaterial filaments through an extruder nozzle using a syringe. The amount of biomaterial deposited is adjusted by displacing a piston. Three-dimensional structures are created by stacking two-dimensional patterns drawn with the filaments.

Bioinks are fluids containing cells that, in bioprinting, are analogous to the inks of paper printers. Biocompatible fluids devoid of cells, which give rise to three-dimensional structures to be populated with cells in later stages of maturation, can also be used and are, according to BioEdTech™ [1] denominated biomaterial inks. Both bioinks and biomaterial inks are usually composed of hydrogels, whose polymeric chains can form cross-links between layers as they are deposited to form solid structures.

Natural cartilaginous extracellular matrices (ECMs) have emerged as promising biomaterials for cartilage reconstitution, partly due to their biochemical complexity that gives them a potentially chondroinductive nature. In this work, some of the studied formulations contained devitalized cartilage (DVC), which is a cartilage ECM whose chondrocytes were destroyed by the formation of ice crystals in freeze/thaw processes, without removing cell debris from within the matrix. Cellular debris can pose a risk of immune response but, according to Farr and Yao [2], cited by Kiyotake *et al.* [3], there is clinical evidence that cartilages are immunoprivileged and,

therefore, the removal of cellular debris may not be necessary.

Pati *et al.* [4] developed a swine-derived cartilage ECM gel, printed together with polycaprolactone (PCL). The ECM of xenogenic origin presented antigenic determinants that could lead to rejection. However, according to Daly *et al.* [5], the effect of those antigens is controversial. Porcine ECM implants in African green monkeys (*Cholrocaebus aethiops*) did result in increased antibody expression, but the implants were well tolerated.

Moutos *et al.* [6] created PCL scaffolds with porcine DVC particles to be seeded with stem cells. However, in that case, a 3D printing technique was not employed. Instead, a miniature weaving loom was used to create 3D constructs woven from PCL multifilament yarns. The constructs were then embedded in a paste containing the swine DVC.

The normal functioning of cells depends, generally, on their anchoring to a substrate. A study by Discher *et al.* [7] on how cells adhere to gels with elasticities similar to those of living tissues have allowed to understand how cells react to the stiffness of the extracellular matrix.

According to Janmey and Schliwa [8], the application of forces external to cells or even the generation of internal forces by adhesion to substrates with different rigidity conditions create signals that can alter the regulation of cellular chemical components. Intracellular signal transduction pathways are connected by adhesion complexes and by the actin and myosin cytoskeleton to structures in the ECM. Thus, the local rigidity of ECM has an influence on cell growth, development, differentiation and multiplication.

Most biomaterials have viscoelastic behavior, which is an intermediate behavior between liquid (viscous) and solid (elastic) behaviors. Consequently, elastic modules and viscosities of those materials as are not constant, but functions of time, pressure and shear.

Biomaterials and biomaterial inks generally need to have low viscosities to pass through the small diameter needles present in the outlets of the bioprinting nozzles. A common property of those materials, which are normally formed by polymers in solution, is shear thinning, which is the decrease in viscosity with the increase in shear stress, and the increase in viscosity with the decrease in shear stress. This is advantageous, as it provides lower viscosities while the materials are subjected to high shear stresses, facilitating the flow during extrusion through bioprinting needles, and the return to higher viscosities when the shear stresses cease, contributing to the material extruded to regain consistency. Moreover, for the construct to acquire the desirable consistency, similar to that of natural tissue, additional crosslinking of the polymer present in the biomaterial can be promoted after bioprinting.

Rheology tests allow determining the shear thinning behavior of each biomaterial by measuring the decrease in absolute viscosity with the increase in shear rate. In this study, data extracted from rheology tests were applied to CFD simulations of extrusion in bioprint nozzles.

CFD simulations are useful for predicting the behavior of biomaterials in bioprinting, preventing the clogging of extruder nozzles and, in cases of biomaterials containing cells (bioinks), also avoiding to waste cells, which could disrupt if subjected to very high shear stresses against the walls of the narrow printing needles.

Blaeser *et al.* [9] concluded that shear stresses below 4 kPa between the walls of extruder nozzles and bioinks would meet satisfactory values, of around 94%, for cell viability after bioprinting. The main objective of this study was to predict the possibility of cell disruption by comparing the calculated shear stresses for novel biomaterials flowing through two different nozzle geometries to the limit of 4 kPa, established by Blaeser *et al.* [9] to meet cell viability.

2 Materials and methods

2.1 Preparation of biomaterial inks

Twelve different biomaterial inks with the potential to be populated with cells to generate bioinks were formulated. The formulations were created from compositions tested by Paxton *et al.* [10], and to some of them were added pulverized DVC and/or granulated PCL. The exogenous pulverized DVC added to the compositions is commercially available and produced by the Tiaraju™ Laboratory (Santo Ângelo, RS, Brazil), under the name of "Cartilagem de Tubarão", from shark cartilage, and has a particle size of 100% below 250 μm, or 60#. PCL in granulated form was obtained through shear comminution, and particle sizes of around 1 mm were obtained. However, 0.41 mm is the largest recommended diameter for filaments in bioprinting, since the diffusion of

oxygen and nutrients through the bioprinted material requires a maximum radius of 0.2 mm to be satisfactory.

The formulations by Paxton *et al.* [10] reproduced for this study are composed as follows.

Poloxamer 407 30% wt. In aqueous solution.

8%/1% alginate. Sodium alginate 8% w/v in phosphate buffered saline (PBS), with pre-crosslinking promoted by 1% w/v $CaCl_2$ solution, mixed with the alginate gel in a proportion of 7: 3 volume mixing ratio.

2%-10% alginate-gelatin. Formulated from a mixture of 4% w/v sodium alginate in PBS and 20% w/v gelatin in PBS (that composition was first tested by Wüst et al. [11] and then reproduced by Paxton et al. [10]).

For biomaterial ink 1, same volumes of the compositions tested by Paxton *et al.* [10] of 8%/1% alginate and of aqueous solution of poloxamer 407 30% wt were mixed. The compositions of biomaterial inks 2, 3 and 4 were variants of the first, with additions of DVC or PCL, according to Tab. 1. Similarly, to the compositions 5 and 9, which were tested by Paxton *et al.* [10], different amounts of DVC or PCL were added to generate the new compositions 6, 7, 8, 10, 11, and 12.

Table 1. Compositions of the biomaterial inks

Biomaterial ink	Compositions
1	8%/1% alginate mixed with poloxamer 407 30% wt in a 1:1 volume mixing ratio
2	Same composition of biomaterial ink 1 with additional DVC 3% wt
3	Same composition of biomaterial ink 1 with additional PCL 3% wt
4	Same composition of biomaterial ink 1 with additional DVC 1.5% wt and PCL 1.5% wt
5	Pure alginate 8%/1%
6	Same composition of biomaterial ink 5 with additional DVC 3% wt
7	Same composition of biomaterial ink 5 with additional PCL 3% wt
8	Same composition of biomaterial ink 5 with additional DVC 1.5% wt and PCL 1.5% wt
9	2% - 10% alginate-gelatin
10	Same composition of biomaterial ink 9 with additional DVC 3% wt
11	Same composition of biomaterial ink 9 with additional PCL 3% wt
12	Same composition of biomaterial ink 9 with additional DVC 1.5% wt and PCL 1.5% wt

2.2 Rheology tests

Rheology tests were performed using a TA Instruments™ AR-G2 rheometer (New Castle, DE) equipped with a Peltier plate and a cone with an angle of 2 degrees.

The tests were carried out at 25°C for compositions corresponding to biomaterial inks numbering 1 to 8, and at 37°C for compositions corresponding to biomaterial inks numbering 9 to 12. The last four, containing gelatin, can be submitted at 37°C in the printheads to take advantage of the gelatin's thermoresponsive character, and then can be cooled between 0 and 4°C right after extrusion to recover consistency.

The absolute viscosity of the different biomaterial inks was measured as a function of the shear rate between 0.003 s^{-1} (the minimum value adopted by Paxton *et al.* [10]) and 2000 s^{-1} (the maximum value adopted by Melchels *et al.* [12]). All compositions showed shear thinning, characterized by a decrease in viscosity with an increasing shear rate.

The Power Law model for the viscosity of non-Newtonian fluids, which exhibit shear thinning behavior, is described by eq. (1):

$$\eta = k \cdot \dot{\gamma}^{n}. \tag{1}$$

η is the absolute viscosity, k is the consistency coefficient, $\dot{\gamma}$ is the shear rate and n is the behavior index, which indicates how much the fluid deviates from the Newtonian model.

The consistency coefficient and the behavior index for each biomaterial ink were calculated using regression equations adjusted to the data of absolute viscosity versus shear rate. The calculated values are listed in Tab. 2. The consistency coefficients reflected the increase in material consistencies by the addition of DVC

and PCL. Behavior indices below 1 for all inks indicated a tendency to shear thinning. Some inks with behavior indices below 1E-08 approach Newtonian behavior.

Table 2. Consistency coefficients and behavior indices calculated for biomaterial inks

Biomaterial ink	k (Pa·s)	n
1	804,8	0,02095
2	1330,0	0,01894
3	9788,0	0,006656
4	3350,0	2,67E-09
5	580,5	0,01325
6	906,0	7,47E-09
7	11050,0	0,03224
8	17430,0	2,78E-07
9	18,1	0,5842
10	434,2	1,46E-08
11	7979,0	3,01E-09
12	9561,0	3,27E-02

2.3 CFD simulations

The simulations were conducted using ANSYS Fluent™ 17.2 (ANSYS, Inc., Canonsburg, PA), with a SIMPLE scheme of pressure-velocity coupling, second order interpolation method for pressure, and second order upwind interpolation method for momentum. Convergence absolute criteria were adopted for continuity, x-velocity and y-velocity equations as 1E-10. Rheometer data of the biomaterial inks were applied to the extrusion process, and the shear effects for the different inks were compared.

The value of 50 microliters per minute for the bioink's volumetric flow rate was adopted after being determined as an intermediate value based on similar values between 35 and 75 microliters reported by Jia *et al.* [13], Dubbin *et al.* [14], and Göhl *et al.* [15]. The outlet pressure was defined as atmospheric.

Two extruder nozzle models, listed as follows, were considered.

A: 0.41 mm outlet diameter. Geometry, shown in Fig. 1, whose needle outlet diameter is the maximum possible so that the diffusion of nutrients and oxygen can be sufficient inside the bioprinted constructs. A mesh size of 1,664,436 elements was adopted.

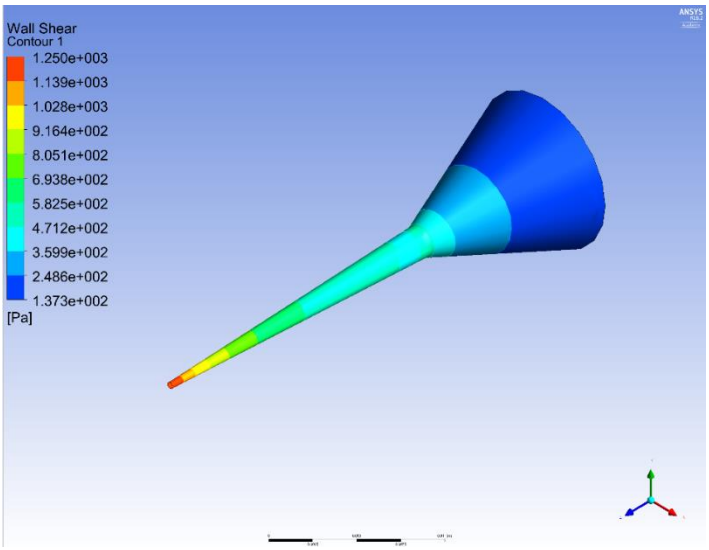

Figure 1. Example of simulation result for geometry A

B: 1.54 mm outlet diameter. Geometry, shown in Fig. 2, whose needle outlet diameter is compatible with the PCL particles (up to 1 mm of diameter) used in the compositions from which the rheology data were obtained. A mesh size of 151,027 elements was adopted (coarser than that of geometry A, because the needle is not as thin).

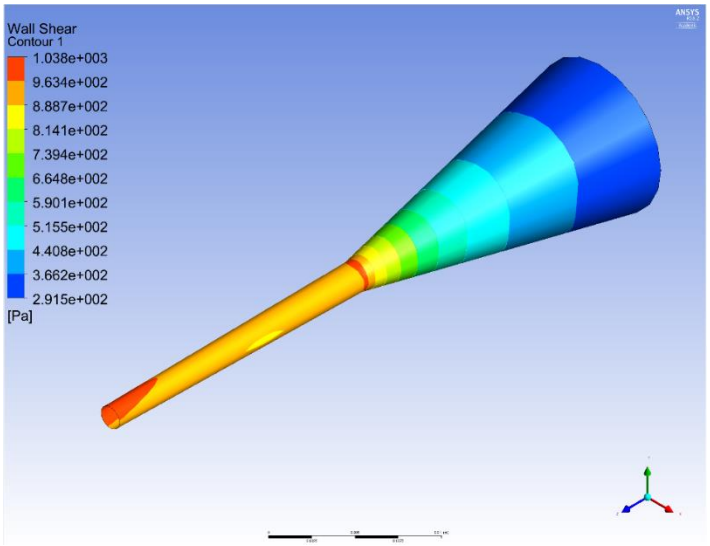

Figure 2. Example of simulation result for geometry B

3 Results and discussion

The data of average and maximum shear stresses obtained for the different biomaterial inks, using geometries A and B, are listed in Tab. 3 and Tab. 4, respectively.

For geometry A, average shear stresses far above 4 kPa were obtained for all compositions containing PCL (inks 3, 4, 7, 8, 11, and 12), which could result in low cell viability if cells were added to the biomaterial prior to extrusion.

The maximum shear stresses were much higher than 4 kPa for all formulations, indicating that, if cell material were added, cell rupture would occur in critical regions of the geometry during extrusion.

Table 3. Average and maximum shear stresses calculated for the different biomaterial inks for geometry A.

Biomaterial ink	Average shear stress (Pa)	Maximum shear stress (Pa)
1	2673	112787
2	4390	184461
3	31458	1284860
4	10616	426806
5	1893	78542
6	2870	115409
7	37554	1627050
8	55228	2220720
9	683	37998
10	1370	55064
11	25152	1011430
12	32375	1404220

For geometry B, average shear stress results were also quite high for compositions containing PCL, except for composition 4. In general, and as expected by the larger diameter of the needle, shear stresses were lower, but the smaller diameter of 0.41 mm is still preferred, as it allows the diffusion of nutrients and oxygen in the constructs. Fig. 2 shows that some obtained wall shear distributions were asymmetric, indicating that the convergence of the models still need to be improved with mesh tests.

Table 4. Average and maximum shear stresses calculated for the different biomaterial inks for geometry B.

Biomaterial ink	Average shear stress (Pa)	Maximum shear stress (Pa)
1	716	4758
2	667	7841
3	8749	56718
4	3001	19231
5	386	3395
6	440	5201
7	10812	94211
8	15466	100053
9	15	229
10	189	1189
11	7132	45579
12	11299	59706

For comparison, Blaeser *et al.* [9] obtained experimental and numerical results for printing alginate at low concentrations (0.5 to 1.5% w/v) with two different nozzle diameters (0.15 mm and 0.30 mm). The average shear stresses calculated at the nozzles varied between 700 Pa and 18 kPa.

To enable the use of the thinnest bioprinting needle (0.41 mm in diameter) in tests containing cell embedded biomaterials, compositions number 6 and number 10 are preferred, because their average shear stresses during extrusion remain below 4kPa, and because they contain DVC, which may bring biochemical and mechanical advantages to the bioprinted constructs.

Compositions containing PCL comminuted in sufficiently small granulometries, for using in bioprinting with 0.41 mm diameter needles, can be considered for the printing of acellular constructs, since in those cases there is no problem in subjecting the materials to high shear stresses during extrusion.

The results of the simulations for the different biomaterial inks have yet to be refined; however, initial estimates indicate inlet pressures above 750 kPa for all compositions while printing with the 0.41 mm diameter needle (considering that the inlet boundary condition was a fixed volumetric flow of 50 microliters per minute). These are not promising estimates for cell viability, compared with the results of Mondal *et al.* [16], who obtained low cell viabilities for even lower inlet pressures, as presented in Tab. 5, while printing alginate and gelatin compositions at room temperature and with a 0.41 mm diameter needle.

Table 5. Correlation of extrusion pressure and cell viability [16]

	Sodium alginate gelatin composition (%w/v)			
	3.25:4	7:3	6:4	4:8
Printing pressure (kPa)	45	115	145	250
Cell viability immediately after printing (approx.)	92%	71%	63%	52%

4 Conclusions

Fluid dynamic simulations indicated the need for very high values of shear stresses during extrusion to enable the flow of biomaterial inks containing PCL. For these compositions, the addition of cellular material after printing the constructs is preferable in relation to the addition to the biomaterial itself before extrusion, as the cell viability after extrusion would be low.

Considering the tests performed, biomaterial inks 6 and 10 presented the best rheological conditions for bioprinting; however, compositions containing PCL in sufficiently small granulometries can provide good results in extrusion and can be considered for the printing of acellular constructs, which can be submitted to high shear stresses during extrusion without concern with cell rupture.

The consistency coefficients calculated showed a gain in consistency of biomaterial inks mainly by adding PCL, but also by adding DVC. Even with the addition of these particulate components, all samples showed shear thinning, reflected in the values of the behavioral indices lower than 1.

The tested compositions of biomaterial inks containing gelatin liquefy at physiological temperature. Thus,

their printed constructs could not be directly implanted in the human body. It is then necessary to discover or develop thermoresponsive polymers with rheological properties similar to those of gelatin that can be photo-crosslinked or chemically crosslinked after bioprinting.

Fluid dynamics simulations applied to different biomaterial inks still need to undergo mesh tests for refinement of the results; however, the meshes already adopted have high orthogonal quality, with minimum values above 0.60 and average values above 0.99, with an ideal value of 1.00. New flow models, which would include the effect of the presence of cells in the biomaterials should be considered.

Acknowledgements. The authors would like to acknowledge the support of Professor Ricardo Geraldo de Sousa and Dr. Cynthia Erbetta, for the opportunity to use rheometer and for their help with its operation.

Authorship statement. The authors hereby confirm that they are the sole liable persons responsible for the authorship of this work, and that all material that has been herein included as part of the present paper is either the property (and authorship) of the authors, or has the permission of the owners to be included here.

References

[1] BioEdTech. *Imersão em Práticas de Bioimpressão* (course handbook), 2019.
[2] J. Farr and J. Q. Yao, "Chondral defect repair with particulated juvenile cartilage allograft". *Cartilage*, vol. 2, pp. 346-353, 2011.
[3] E. A. Kiyotake, E. C. Beck and M. S. Detamore, "Cartilage extracellular matrix as a biomaterial for cartilage regeneration". *Annals of the New York Academy of Sciences, Musculoskeletal Repair and Regeneration*, pp. 139-159, 2016.
[4] F. Pati, J. Jang, D. H. Ha, S. W. Kim, J. W. Rhie, J. H. Shim, D. H. Kim and D. W. Cho, "Printing three-dimensional tissue analogues with decellularized extracellular matrix bioink". *Nature Communications*, vol. 5, n. 3935, 2014.
[5] K. A. Daly, A. A. Stewart-Akers, K. Cordero, S. A. Johnson and S. F. Badylak. "The effect of the αGal epitope in the response to ECM in a nonhuman primate model". *The Journal of Immunology*, vol. 182, n 141.26, 2009.
[6] F. T. Moutos, B. T. Estes and F. Guilak, "Multifunctional Hybrid Three-dimensionally Woven Scaffolds for Cartilage Tissue Engineering". *Macromolecular Bioscience*, vol. 10, pp. 1355-1364, 2010.
[7] D. E. Discher, P. Janmey and Y. L. Wang, "Tissue Cells Feel and Respond to the Stiffness of Their Substrate". *Science*, vol. 310, 5751st ed., pp. 1139-1143, 2005.
[8] P. A. Janmey and M. Schliwa, "Rheology". *Current biology*, vol. 18, 15st ed., pp. 639-641, 2008.
[9] A. Blaeser, D. F. D. Campos, U. Puster, W. Richtering, M. M. Stevens and H. Fischer, "Controlling Shear Stress in 3D Bioprinting is a Key Factor to Balance Printing Resolution and Stem Cell Integrity". *Advanced Healthcare Materials*, 2016.
[10] N. Paxton, W. Smolan, T. Bock, F. Melchels, J. Groll and T. Jungst, "Proposal to assess printability of bioinks for extrusion-based bioprinting and evaluation of rheological properties governing bioprintability". *Biofabrication*, vol. 9, 2017. doi: 10.1088/1758-5090/aa8dd8
[11] S. Wust, R. Muller and S. Hofmann, "3D Bioprinting of complex channels-effects of material, orientation, geometry, and cell embedding". *Journal of Biomedical Material Research A*, vol. 103, pp. 2558-2570, 2015.
[12] F. P. W. Melchels, M. M. Blokzij, R. Levato, Q. C. Peiffer, M. Ruijter, W. E. Hennink, T. Vermonden and J. Malda, "Hydrogel-based reinforcement of 3D bioprinted constructs". *Biofabrication*, vol. 8, 3st ed., 2016.
[13] W. Jia, P. Gungor-Ozkerim, Y. Zhang, K. Yue, K. Zhu, W. Liu, Q. Pi, B. Byambaa, M. Dokmeci, S. Shin and A. Khademhosseini. "Direct 3D bioprinting of perfusable vascular constructs using a blend bioink". *Biomaterials*, vol. 106, pp. 58-68, 2016.
[14] K. Dubbin, A. Tabet and S. Heilshorn, "Quantitative criteria to benchmark new and existing bio-inks for cell compatibility". *Biofabrication*, vol. 9, doi: https://doi.org/10.1088/1758-5090/aa869f, 2017.
[15] J. Gohl, K. Markstedt, A. Mark, K. Hakansson, P. Gatenholm and F. Edelvik, "Simulations of 3D bioprinting: predicting bioprintability of nanofibrillar inks". *Biofabrication*, vol. 10, doi: https://doi.org/10.1088/1758-5090/aac872, 2018.
[16] A. Mondal, A. Gebeyehu, M. Miranda, D. Bahadur, N. Patel, S. Ramakrishnan, A. K. Rishi and M. Singh, "Characterization and printability of Sodium alginate-Gelatin hydrogel for bioprinting NSCLC co-culture". *Nature Research Scientific Reports*, vol. 9:19914, 2019.